ORIGINAL RESEARCH

Feasibility and Accuracy of Cardiac Magnetic Resonance Imaging–Based Whole-Heart Inverse Potential Mapping of Sinus Rhythm and Idiopathic Ventricular Foci

Pranav Bhagirath, MD; Maurits van der Graaf, MD; Elise van Dongen, MD; Jacques de Hooge, MSc; Vincent van Driel, MD; Hemanth Ramanna, MD, PhD; Natasja de Groot, MD, PhD; Marco J. W. Götte, MD, PhD

***Background*—**Inverse potential mapping (IPM) noninvasively reconstructs cardiac surface potentials using body surface potentials. This requires a volume conductor model (VCM), usually constructed from computed tomography; however, computed tomography exposes the patient to harmful radiation and lacks information about tissue structure. Magnetic resonance imaging (MRI) is not associated with this limitation and might have advantages for mapping purposes. This feasibility study investigated a magnetic resonance imaging–based IPM approach. In addition, the impact of incorporating the lungs and their particular resistivity values was explored.

***Methods and Results*—**Three volunteers and 8 patients with premature ventricular contractions scheduled for ablation underwent 65-electrode body surface potential mapping. A VCM was created using magnetic resonance imaging. Cardiac surface potentials were estimated from body surface potentials and used to determine the origin of electrical activation. The IPM-defined origin of sinus rhythm corresponded well with the anatomic position of the sinus node, as described in the literature. In patients, the IPM-derived premature ventricular contraction focus was 3-dimensionally located within 8.3±2.7 mm of the invasively determined focus using electroanatomic mapping. The impact of lungs on the IPM was investigated using homogeneous and inhomogeneous VCMs. The inhomogeneous VCM, incorporating lung-specific conductivity, provided more accurate results compared with the homogeneous VCM (8.3±2.7 and 10.3±3.1 mm, respectively; P=0.043). The interobserver agreement was high for homogeneous (intraclass correlation coefficient 0.862, P=0.003) and inhomogeneous (intraclass correlation coefficient 0.812, P=0.004) VCMs.

***Conclusion*—**Magnetic resonance imaging–based whole-heart IPM enables accurate spatial localization of sinus rhythm and premature ventricular contractions comparable to electroanatomic mapping. An inhomogeneous VCM improved IPM accuracy. **(*J Am Heart Assoc*. 2015;4:e002222 doi: 10.1161/JAHA.115.002222)**

Key Words: cardiac magnetic resonance imaging • catheter ablation • noninvasive cardiac imaging • premature ventricular contractions

Inverse potential mapping (IPM) allows for noninvasive reconstruction of epicardial activation patterns. The most frequently used IPM method is based on a homogeneous volume conductor model (VCM) constructed from computed tomography images.[1] This technique is being applied increasingly for analysis of idiopathic ventricular foci and guidance of catheter ablation.[2,3]

Although clinically useful, this computed tomography–based approach has important limitations. The most important limitation, besides the exposure to radiation and associated risk of malignancies,[4] is the inability to characterize tissue in detail. Magnetic resonance imaging (MRI) does not have these limitations and is considered the gold standard for tissue characterization, in particular for edema and fibrosis. Although most publications underscore the fact that both computed tomography and MRI can be used, MRI is less frequently used for IPM.[5–7]

In addition, the use of a homogeneous VCM could also be considered a limitation because it may not appropriately incorporate the effects of specific tissue-conductivity characteristics such as those from the lungs (ie, inhomogeneous conditions).[8]

From the Department of Cardiology, Haga Teaching Hospital, The Hague, The Netherlands (P.B., M.G., E.D., J.H., V.D., H.R., M.J.W.G.); Department of Cardiology, Erasmus Medical Centre, Rotterdam, The Netherlands (N.G.).

Accompanying Videos S1 and S2 are available at http://jaha.ahajournals.org/content/4/10/e002222/suppl/DC1

Correspondence to: Marco J. W. Götte, MD, PhD, Department of Cardiology, HAGA Teaching Hospital, Leyweg 275, 2545CH The Hague, The Netherlands. E-mail: mjw.gotte@hagaziekenhuis.nl

Received June 29, 2015; accepted August 12, 2015.

This study investigated the feasibility of whole-heart IPM using a VCM derived from MRI. The clinical applicability of this approach was evaluated in healthy volunteers and patients with idiopathic ventricular foci. In addition, the influence of tissue impedance on the results of IPM was studied using 2 different VCMs. A homogeneous thoracic VCM (model 1) was compared with an inhomogeneous VCM in which, in addition to thoracic impedance, the resistance value of the lungs was included (model 2).

Methods

Patient Population

The study population consisted of 3 healthy volunteers and 8 patients with symptomatic or therapy-resistant premature ventricular contractions (PVCs). The study complied with the Declaration of Helsinki and received approval from the local ethics committee (METC Zuidwest Holland study NL38156.098.11) and the institutional scientific board. Written informed consent was obtained from the study participants.

Body Surface Potential Acquisition

An MRI scout scan was performed to approximate the position of the heart with respect to the thorax. Subsequently, 62 (+3 limb) electrodes were applied to each participant's torso, centralized over the heart. Body surface potentials (BSPs) were acquired using a 65-channel ActiveTwo system (BioSemi BV). Once the acquisition was completed, the electrode locations were marked with MRI markers, enabling accurate identification of the electrode positions.

Image Acquisition

MRI studies were obtained using a 1.5T Aera scanner (Siemens Healthcare). Blackblood imaging was performed using a half-Fourier acquisition single-shot turbo spin-echo, or HASTE, pulse sequence to acquire 3 perpendicular stacks (axial, coronal, and sagittal) from the neck to the lower abdomen.

Images were acquired during free breathing using navigator gating (diaphragm) with a 1-mm window. ECG gating was used to acquire images during the diastolic phase of the cardiac cycle. Typical imaging parameters were spatial resolution of $1.2\times1.2\times6$ mm, repetition time/echo time 744/42 ms, and flip angle of 160°.

VCM and Computational Algorithm

The MRI images were segmented using a custom-developed tool. This tool generates a script containing the geometric description (points, lines and planes, and directed line loops) of the segmentation. Subsequently, the script was meshed using GMSH.[9] Conductivity for the homogeneous VCM (model 1) was specified at 0.2 Siemens per meter (S/m).[10] The inhomogeneous VCM (model 2) had a similar summation but also contained specific conductivity values for the lungs, specified at 0.04 S/m.[10]

Cardiac surface potentials were calculated from BSPs using the following equation in which CSP indicates cardiac surface potentials, T is the transfer matrix, and λ is the regularization strength:

$$\mathrm{CSP} = (\mathrm{T}^{\mathrm{T}}\,\mathrm{T} + \lambda^2\,\mathrm{I})^{-1}\,\mathrm{T}^{\mathrm{T}}\,\mathrm{BSP}$$

Electrophysiological Study and Catheter Ablation

The electrophysiologists (H.R. and V.D.) were blinded to the IPM results. During the electrophysiological study, femoral venous and arterial access was established. In all cases, a hexapolar catheter (Supreme; St. Jude Medical) was placed in the right atrial appendage, and the proximal electrode located in the inferior vena cava served as the unipolar indifferent electrode. In addition, a screw-in temporary pacing lead (Medtronic) was placed in the right ventricle as a positional reference for the electroanatomic mapping (EAM) system (Ensite Velocity 3.0; St. Jude Medical). An EAM was created using the roving catheter. Respiratory compensation was set to automatic. No field scaling was performed.

If no spontaneous PVCs were present, isoproterenol and/or pacing maneuvers were used to provoke PVCs. After the focus location was identified, targeted ablation was performed using a standard 4-mm nonirrigated ablation catheter with power delivery up to 50 W and a temperature limitation of 50°C. Subsequently, the site of ablation was marked on the EAM system.

Comparison of Focus Localization

Following the ablation procedure, the ectopic PVC focus location identified on the IPM was compared with the site of ablation specified on the EAM (gold standard). For this purpose, 2 experienced operators (P.B. and H.R.) independently identified the foci on IPM and EAM to provide a measure of interobserver variability.

This approach resulted in 3 different data sets describing the focus localization as the *x, y*, and *z* coordinates: (1) IPM using the homogeneous model (data set 1), (2) IPM using the inhomogeneous model (data set 2), and (3) EAM (data set 3). Subsequently, Pythagoras' theorem for 3-dimensional coordinate vectors, in which the distance between 2 points is equal to the square root of the sum of the squared coordinate differences, was used to calculate the differences between coordinate data sets 1 and 3 and coordinate data sets 2 and 3.

Statistical Analysis

Statistical analysis was performed using IBM SPSS Statistics (version 22.0; IBM Corp). Continuous variables were expressed as mean±SD or as median and interquartile range. Localization errors between the 2 VCMs were compared using the Wilcoxon signed-rank test. The intraclass correlation coefficient was used to analyze interobserver agreement. $P<0.05$ was considered statistically significant.

Results

Study Population

Baseline characteristics of the 3 volunteers and 8 patients (N=11) are provided in Table 1. All volunteers had normal ECGs. In both volunteers and patients, structural heart disease was excluded based on the MRI examination.

Ablation Procedure

The preprocedural median PVC burden was 14 121 ectopic beats per 24 hours (interquartile range 10 432 to 22 373 ectopic beats per 24 hours). Average procedural time, including mapping and ablation, was 129±53 minutes. An average of 4468 points were acquired to construct the EAM. No periprocedural displacements of the EAM were observed.

After catheter ablation, the PVC burden was reduced to a median of 17 ectopic beats per 24 hours (interquartile range 1 to 24 ectopic beats per 24 hours), a reduction of >99%.

Table 1. Characteristics of Participants Undergoing Inverse Potential Mapping

	Volunteers	Patients
n	3	8
Age, y	28±3	46±13
BMI	22.1±1.4	25.2±6.7
Female (%)	1 (33)	7 (88)
LVEF (%)	55±2	50±3
RVOT PVCs	—	6 (75%)
Duration of PVCs, months	—	18±12
PVC burden before procedure	—	14 121 (10 432 to 22 373)
PVC burden after procedure	—	17 (1 to 24)

Age, BMI, LVEF, and PVC duration are expressed in mean±SD. PVC burden before and after procedure is expressed using median (interquartile range). PVC burden is expressed in ectopic beats per 24 hours. BMI indicates body mass index; LVEF, left ventricular ejection fraction; PVC, premature ventricular contractions; RVOT, right ventricular outflow tract.

IPM in Sinus Rhythm

During sinus rhythm, the first point of activation on the potential map of healthy volunteers was located anatomically near the transition of the superior vena cava (crista terminalis) into the right atrium (Figure 1A, white arrow). Ventricular breakthrough began at the right ventricular free wall (Figure 1B), at the site at which the moderator band was attached to the ventricular myocardium.

Comparison Between IPM Focus and Actual Ablation Site

No pacing maneuvers were required for PVC induction. Five patients required isoproterenol to induce PVCs. Based on invasive mapping, the ablation site was in the right ventricular outflow tract (VOT) in 6 patients and in the left VOT in 2 patients (Table 2). One patient had a right bundle branch block, which was reconstructed correctly by IPM (Video S1).

In all 8 cases, IPM located the ectopic focus in the correct cardiac compartment (Table 2). IPM identified all right VOT foci in close proximity to the ablation lesion (8.4±3 mm, n=6) defined on the EAM (Figure 2; Video S2). A similar difference was found for the left VOT foci (7.9±1.5 mm, n=2). IPM located 1 of the left VOT foci (Case 2) at the right coronary cusp; however, the ablation for this patient was performed successfully in the distal left VOT (Figure 3). The other left VOT focus was closely approximated to the actual site of ablation.

Comparison Between Homogeneous and Inhomogeneous VCMs

The comparison of PVC focus between the inhomogeneous VCM and EAM demonstrated localization accuracy of 8.3±2.7 mm (observer 1) and 8.2±2.8 mm (observer 2), with high interobserver agreement (intraclass correlation coefficient 0.812, 95% CI 0.318 to 0.959, $P=0.004$). A similar comparison between the homogeneous VCM and EAM demonstrated accuracy of 10.3±3.1 mm (observer 1) and 9.8±2.9 mm (observer 2) and also showed high interobserver agreement (intraclass correlation coefficient 0.862, 95% CI 0.399 to 0.975, $P=0.003$).

The focus localization accuracy showed significant differences between the homogeneous and inhomogeneous VCMs. The homogeneous VCM had a significantly higher localization error compared with the inhomogeneous VCM for both observers ($P=0.043$) (Table 3). In addition, the homogeneous VCM failed to identify the focus in 1 right VOT case (Figure 4, case 6), in which the inhomogeneous model correctly identified the site of ablation.

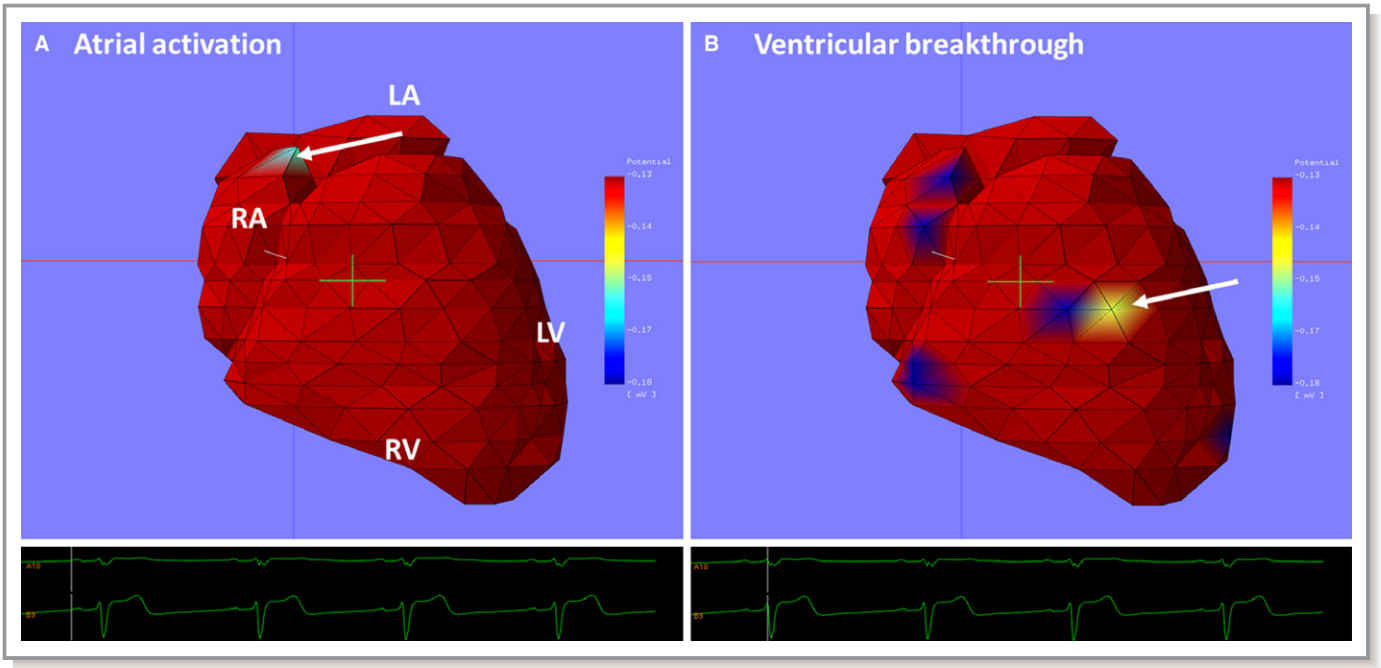

Figure 1. IPM in a healthy volunteer during sinus rhythm. The left panel depicts the IPM at the start of the atrial depolarization (P wave), and the right panel depicts the IPM at the start of the ventricular depolarization (QRS). The anterior-posterior view of the 3-dimensional heart model can be observed. The first point of atrial activation is observed near the entrance of the superior vena cava (white arrow) into the right atrium. The first point of ventricular activation is observed at the RV free wall (white arrow), at which the moderator band is attached to the ventricular myocardium. IPM indicates inverse potential mapping; LA, left atrium; LV, left ventricle; RA, right atrium; RV, right ventricle.

Discussion

To our knowledge, this study is the first to investigate whole-heart IPM using a 62-lead anterior BSP recording and an MRI-derived inhomogeneous VCM.

The evaluation of this model was performed in healthy volunteers and patients with idiopathic arrhythmias. Using this MRI-based noninvasive method, it was possible to estimate the PVC focus location with clinically sufficient accuracy using BSPs of a single ectopic beat. In addition, a comparison between 2 independent observers demonstrated high reproducibility of the results.

Table 2. Comparison of PVC Focus Identified With IPM and Ablation Site on Electroanatomic Mapping

Case	PVC Focus IPM	Ablation Site
1	NCC–LCC junction	LCC
2	RVOT-septal	RVOT-septal
3	RVOT-anterior proximal	RVOT-anterior proximal
4	RVOT-anterior	RVOT-anterior
5	RVOT-septal proximal	RVOT-septal proximal
6	RVOT-anteroseptal	RVOT-septal
7	RVOT-posteroseptal	RVOT-septal
8	NCC	NCC

LCC indicates left coronary cusp; LVOT, left ventricular outflow tract; NCC, non-coronary cusp; RCC, right coronary cusp; RVOT, right ventricular outflow tract.

Evaluation in Healthy Volunteers

IPM localized the origin of atrial activity near the transition of the superior vena cava (crista terminalis) into the right atrium. This location has been described in the literature as the anatomic location of the sinus node.[11] These results suggest that atrial activity may be assessed noninvasively using this combined MRI–IPM method.

The first ventricular epicardial breakthrough was located at the right ventricular free wall and corresponded with descriptions in the literature.[1,12] Furthermore, it was also possible to visualize abnormal ventricular activation patterns such as a right bundle branch block (Video S1).

These findings illustrate the potential sensitivity of IPM to detect minute changes in cardiac activation and demonstrate the ease of combining IPM with MRI acquisitions. This result offers the prospect of using this method for screening purposes.

Clinical Impact in Idiopathic PVC Ablation

IPM successfully approximated the ablation site in 8 of 8 patients, providing a surrogate for the clinical PVC focus.

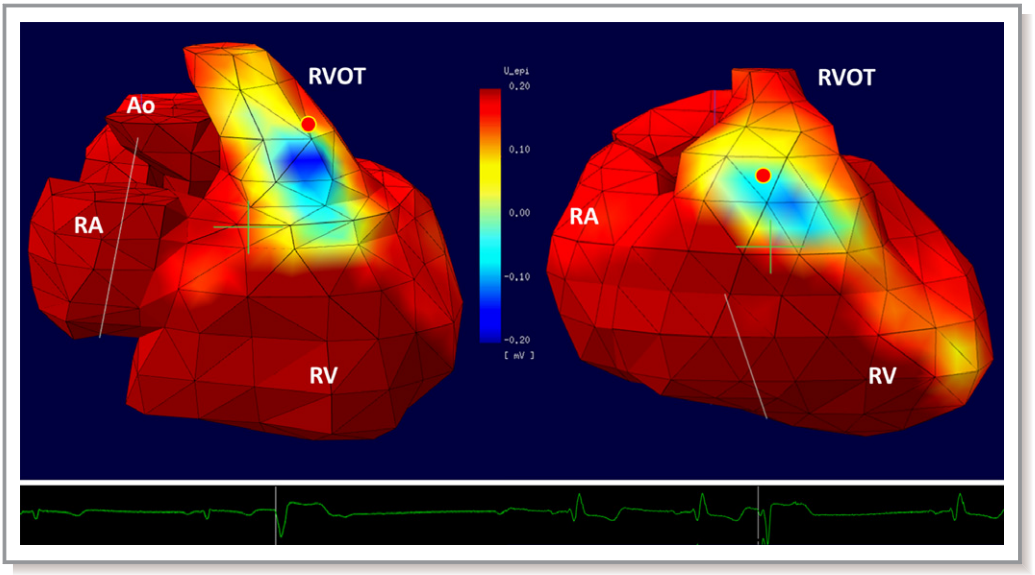

Figure 2. Comparison between inverse potential mapping and electroanatomic mapping for patients with RVOT premature ventricular contractions. Blue indicates the area of epicardial breakthrough. The red dot indicates the site of ablation. ECG is provided underneath each image. Ao indicates the aorta; RA, right atrium; RV, right ventricle; RVOT, right ventricular outflow tract.

This finding suggests that routine application of this noninvasive technique as part of the clinical workup could have multiple benefits such as improved ablation planning due to accurate preprocedural identification of the PVC focus (target ablation site) and reduction in procedural duration (and accompanying radiation exposure) due to reduced invasive mapping time. This may especially be valid for patients with a low PVC burden and/or multifocal PVCs.

Volume Conductor Models

The current, most frequently used BSP mapping technique (ECVUE; CardioInsight Technologies Inc) uses a homogeneous torso conductor model. The clinical utility of this method has been demonstrated after extensive investigation[13,14]; however, recent research advocates the integration of the various organs with their own specific impedance.[8,15] This may be the case particularly in patients with high body surface area,

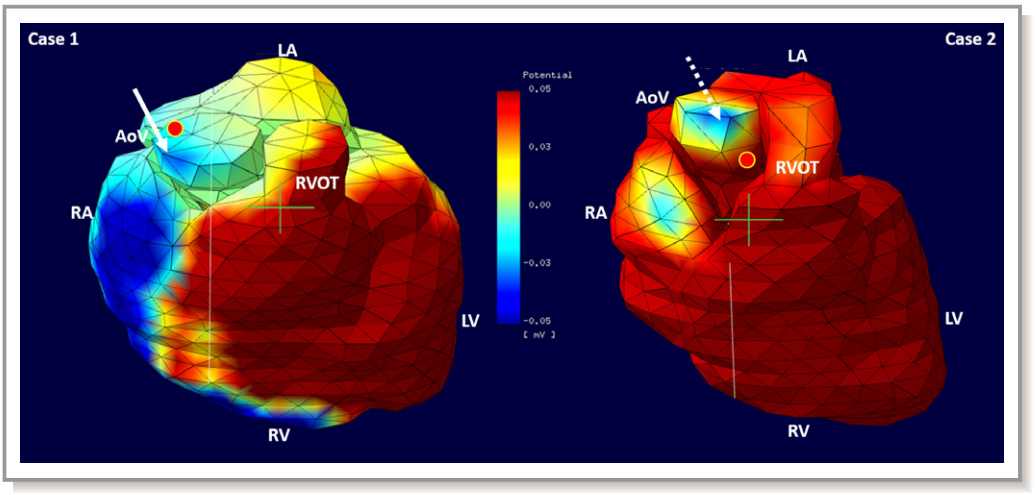

Figure 3. Comparison between inverse potential mapping and electroanatomic mapping for the patients with left ventricle outflow tract premature ventricular contractions. Blue indicates the area of epicardial breakthrough (white arrows). The red dot indicates the site of ablation. ECG is provided underneath each image. AoV indicates the aortic valve; LA, left atrium; LV, left ventricle; RA, right atrium; RV, right ventricle; RVOT, right ventricular outflow tract.

Table 3. Localization Difference Between Ectopic Focus Identified Using Homogeneous and Inhomogeneous Volume Conductor Model Compared With the Ablation Site Marked on the Electroanatomic Mapping

Case	Homogeneous (mm)	Inhomogeneous (mm)	*P* Value
1	11.1	9.3	
2	9.1	9.1	
3	6.4	6.4	
4	14.4	12.1	
5	Focus not identified	7.6	
6	14.9	11.7	
7	7.8	3.6	
8	8.3	6.4	
Median (IQR)	9.1 (7.8 to 14.4)	8.35 (6.4 to 11.1)	*P*=0.043

IQR indicates interquartile range.

pulmonary edema, or myocardial infarction. These circumstances could substantially influence the BSPs due to altered conductivity and resistivity conditions.

The comparison performed in this study indicated a significant difference between homogeneous and inhomogeneous VCMs (Table 3). These results suggest that although it is possible to perform IPM using a homogeneous VCM, an inhomogeneous VCM provides more accurate results.

Limitations

Several inherent technical limitations may have led to the observed differences between IPM-identified ectopic focus and site of ablation defined on the EAM.

Although clinically more practical, the limited number of electrodes used in this study and the electrode positioning on the patient thorax may have affected the accuracy of focus localization. In addition, movement of the ablation catheter may cause spatial displacement of the marked ablation site by ≈10 mm.[16] Furthermore, small and subtle catheter movements can also result in significant shifts within the EAM while using a reference catheter. All of these factors could have contributed to the differences in focus location between IPM and EAM.

Even if these conditions can be optimized, factors still remain that may cause discrepancies. These include image misregistration due to patient respiration, inaccurate cardiac geometry due to image acquisition during different phases of the cardiac cycle, and substantial regional variations in

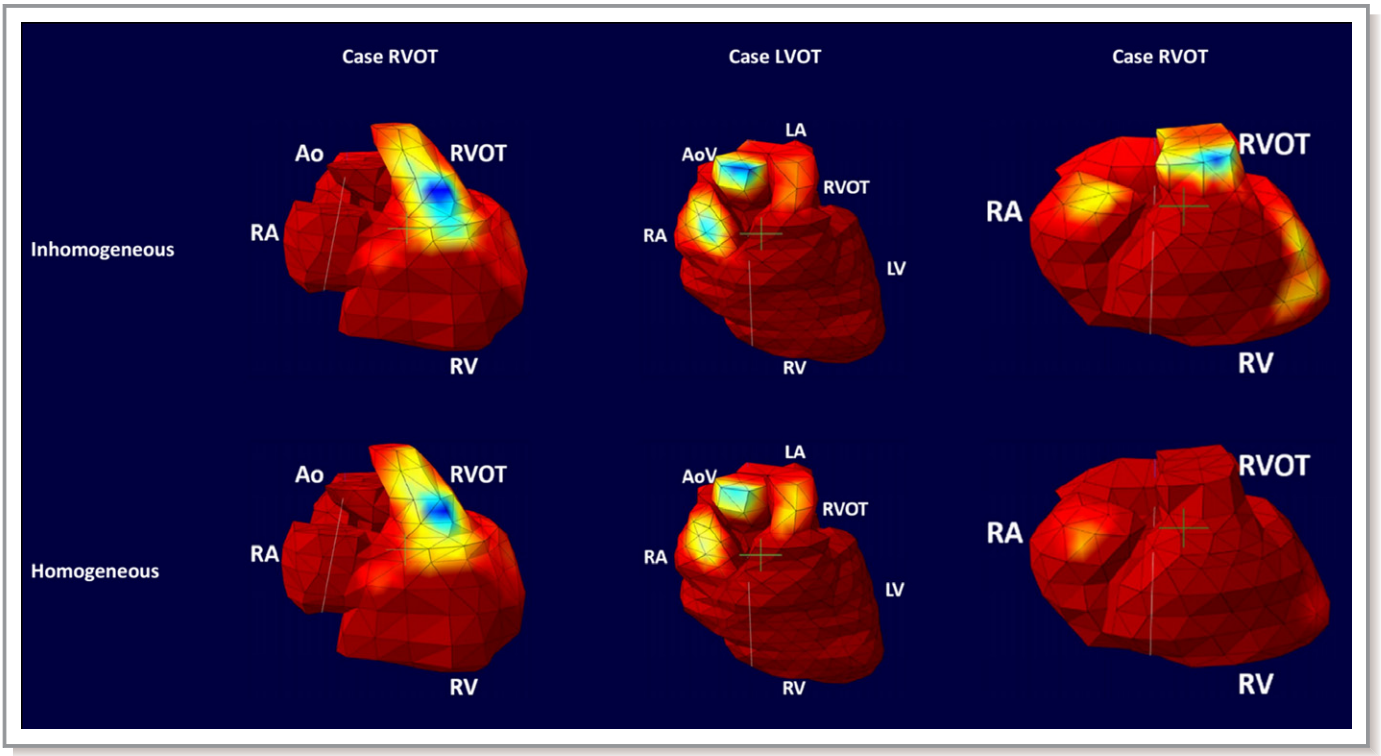

Figure 4. Comparison between homogeneous and inhomogeneous VCMs. Left and center columns depict insignificant and subtle differences between homogeneous and inhomogeneous VCMs, respectively. The right column depicts a clinically significant difference between the 2 VCMs. Ao, indicates the aorta; AoV, aortic valve; LA, left atrium; LV, left ventricle; LVOT indicates left ventricular outflow tract; RA, right atrium; RV, right ventricle; RVOT, right ventricular outflow tract; VCM, volume conductor model.

cardiac displacement during contraction and relaxation (ranging between 5 and 25 mm).[17,18] In particular, the base of the heart moves ≥20 mm toward the apex. This is of particular importance because all ectopic foci were located at the basal part of the heart. Motion-related inaccuracies will probably have less influence on hearts with reduced function (less movement) or when analyzing foci from regions less susceptible to motion. A larger study will be needed to establish the impact of a screening approach prior to routine implementation.

Future Directions

This proposed strategy combining IPM and MRI offers the prospect of studying electrical activation in relation to tissue characteristics for complex ventricular or supraventricular tachycardias and scar-based arrhythmias with clinically relevant accuracy.

The design of the computational model allows for instantaneous integration of patient-specific characteristics such as tissue properties and their associated conductivity. These tissue properties can be obtained easily using MRI. Integration of these characteristics will enable the operator to provide more patient-tailored therapy.

Conclusion

This study demonstrates the clinical applicability of an MRI-based whole-heart IPM method in patients with idiopathic ventricular foci. There was high localization accuracy between the focus identified with IPM and the ablation site on the EAM. The interobserver agreement was high for both VCMs. IPM accuracy improved significantly when using an inhomogeneous VCM.

The integration of this IPM technique with EAM systems may facilitate patient-specific catheter-ablation strategies.

Sources of Funding

Research grants are provided by St Jude Medical and Medtronic NL.

Disclosures

None.

References

1. Ramanathan C, Ghanem RN, Jia P, Ryu K, Rudy Y. Noninvasive electrocardiographic imaging for cardiac electrophysiology and arrhythmia. *Nat Med*. 2004;10:422–428.
2. Jamil-Copley S, Bokan R, Kojodjojo P, Qureshi N, Koa-Wing M, Hayat S, Kyriacou A, Sandler B, Sohaib A, Wright I, Davies DW, Whinnett Z, Peters S, Kanagaratnam P, Lim PB. Noninvasive electrocardiographic mapping to guide ablation of outflow tract ventricular arrhythmias. *Heart Rhythm*. 2014;11:587–594.
3. Erkapic D, Greiss H, Pajitnev D, Zaltsberg S, Deubner N, Berkowitsch A, Mollman S, Sperzel J, Rolf A, Schmitt J, Hamm C, Kuniss M, Neumann T. Clinical impact of a novel three-dimensional electrocardiographic imaging for non-invasive mapping of ventricular arrhythmias-a prospective randomized trial. *Europace*. 2015;17:591–597.
4. Roguin A. CardioPulse. Radiation in cardiology: can't live without it!: using appropriate shielding, keeping a distance as safely as possible and reducing radiation time are essential principles for radiation reduction. *Eur Heart J*. 2014;35:599–600.
5. van Dam PM, Tung R, Shivkumar K, Laks M. Quantitative localization of premature ventricular contractions using myocardial activation ECGI from the standard 12-lead electrocardiogram. *J Electrocardiol*. 2013;46:574–579.
6. Cochet H, Dubois R, Sacher F, Derval N, Sermesant M, Hocini M, Montaudon M, Haissaguerre M, Laurent F, Jais P. Cardiac arrythmias: multimodal assessment integrating body surface ECG mapping into cardiac imaging. *Radiology*. 2014;271:239–247.
7. Revishvili AS, Wissner E, Lebedev DS, Lemes C, Deiss S, Metzner A, Kalinin VV, Sopov OV, Labartkava EZ, Kalinin AV, Chmelevsky M, Zubarev SV, Chaykovskaya MK, Tsiklauri MG, Kuck KH. Validation of the mapping accuracy of a novel non-invasive epicardial and endocardial electrophysiology system. *Europace*. 2015;17:1282–1288.
8. Bear LR, Cheng LK, LeGrice IJ, Sands GB, Lever NA, Paterson DJ, Smaill BH. The forward problem of electrocardiography: is it solved? *Circ Arrhythm Electrophysiol*. 2015;8:677–684.
9. Marchandise E, Geuzaine C, Remacle JF. Cardiovascular and lung mesh generation based on centerlines. *Int J Numer Method Biomed Eng*. 2013;29:665–682.
10. Oostendorp T, Nenonen J, Korhonen P. Noninvasive determination of the activation sequence of the heart: application to patients with previous myocardial infarctions. *J Electrocardiol*. 2002;35(suppl):75–80.
11. Sanchez-Quintana D, Cabrera JA, Farre J, Climent V, Anderson RH, Ho SY. Sinus node revisited in the era of electroanatomical mapping and catheter ablation. *Heart*. 2005;91:189–194.
12. Arisi G, Macchi E, Baruffi S, Spaggiari S, Taccardi B. Potential fields on the ventricular surface of the exposed dog heart during normal excitation. *Circ Res*. 1983;52:706–715.
13. Ramanathan C, Rudy Y. Electrocardiographic imaging: I. Effect of torso inhomogeneities on body surface electrocardiographic potentials. *J Cardiovasc Electrophysiol*. 2001;12:229–240.
14. Ramanathan C, Rudy Y. Electrocardiographic imaging: II. Effect of torso inhomogeneities on noninvasive reconstruction of epicardial potentials, electrograms, and isochrones. *J Cardiovasc Electrophysiol*. 2001;12:241–252.
15. van Oosterom A. A comparison of electrocardiographic imaging based on two source types. *Europace*. 2014;16(suppl 4):iv120–iv128.
16. Andreu D, Berruezo A, Fernandez-Armenta J, Herczku C, Borras R, Ortiz-Perez JT, Mont L, Brugada J. Displacement of the target ablation site and ventricles during premature ventricular contractions: relevance for radiofrequency catheter ablation. *Heart Rhythm*. 2012;9:1050–1057.
17. Zwanenburg JJM, Gotte MJW, Kuijer JPA, Hofman MBM, Knaapen P, Heethaar RM, van Rossum AC, Marcus JT. Regional timing of myocardial shortening is related to prestretch from atrial contraction: assessment by high temporal resolution MRI tagging in humans. *Am J Physiol Heart Circ Physiol*. 2005;288:H787–H794.
18. ter Keurs HE, Rijnsburger WH, van Heuningen R, Nagelsmit MJ. Tension development and sarcomere length in rat cardiac trabeculae. Evidence of length-dependent activation. *Circ Res*. 1980;46:703–714.